Research Article

Niusha Mesgaribarzi*, Youcef Djenouri, Ahmed Nabil Belbachir, Tomasz Michalak, and Gautam Srivastava

# Intelligent explainable optical sensing on Internet of nanorobots for disease detection

https://doi.org/10.1515/ntrev-2024-0019
received September 26, 2023; accepted April 2, 2024

**Abstract:** Combining deep learning (DL) with nanotechnology holds promise for transforming key facets of nanoscience and technology. This synergy could pave the way for groundbreaking advancements in the creation of novel materials, devices, and applications, unlocking unparalleled capabilities. In addition, monitoring psychological, emotional, and physical states is challenging, yet recent advancements in the Internet of Nano Things (IoNT), nano robot technology, and DL show promise in collecting and processing such data within home environments. Using DL techniques at the edge enables the processing of Internet of Things device data locally, preserving privacy and low latency. We present an edge IoNT system that integrates nanorobots and DL to identify diseases, generating actionable reports for medical decision-making. Explainable artificial intelligence enhances model transparency, aiding clinicians in understanding predictions. Intensive experiments have been carried out on Kvasir dataset to validate the applicability of the designed framework, where the accuracy of results demonstrated its potential for in-home healthcare management.

**Keywords:** deep learning, Internet of nano thing, XAI, disease detection, nanorobots

*** Corresponding author: Niusha Mesgaribarzi,** Department of Microsystems, University of South-Eastern Norway, Kongsberg, Norway, e-mail: niusha@ieee.org
**Youcef Djenouri:** Department of Microsystems, University of South-Eastern Norway, Kongsberg, Norway; Norwegian Research Centre, Oslo, Norway; IDEAS NCBR, Warsaw, Poland,
e-mail: youcef.djenouri@usn.no, yodj@norceresearch.no
**Ahmed Nabil Belbachir:** Norwegian Research Centre, Oslo, Norway,
e-mail: nabe@norceresearch.no
**Tomasz Michalak:** IDEAS NCBR, Warsaw, Poland,
e-mail: tomasz.michalak@ideas-ncbr.pl
**Gautam Srivastava:** Department of Mathematics and Computer Science, Brandon University, Brandon R7A 6A9, Canada; Research Center for Interneural Computing, China Medical University, Taichung 40402, Taiwan, Republic of China, e-mail: srivastavag@brandonu.ca

## 1 Introduction

The integration of deep learning (DL) with nanotechnology has the potential to revolutionize various aspects of nanoscience and nanotechnology, leading to the development of new materials, devices, and applications with unprecedented capabilities [1]. In addition, development of sensing technologies has significantly transformed various industries, enabling precise measurements, real-time monitoring, enhanced data analysis, and user-customized design [2–5]. Optical sensors, in particular, have played a crucial role in sensing applications due to their high sensitivity, fast response, and non-invasive nature. With recent advancements in artificial intelligence (AI) and machine learning, the integration of these technologies with optical sensors has paved the way for next-generation smart sensors capable of intelligent and autonomous operation [6–8]. Optical sensors operate based on the interaction of light with the target material, allowing for the detection and quantification of physical, chemical, or biological parameters. These sensors use a range of optical phenomena, including absorption, fluorescence, scattering, and refractive index changes, to capture valuable information from the sensing environment. Traditionally, optical sensors relied on predefined algorithms for data interpretation, limiting their adaptability and flexibility in dynamic sensing scenarios [9]. However, the integration of AI techniques, such as machine learning and DL, with optical sensors has revolutionized their capabilities. Machine learning algorithms empower optical sensors to learn from data, recognize patterns, and make predictions or classifications. DL, a subset of machine learning, uses neural networks to extract intricate features and patterns from complex datasets. By combining AI with optical sensor systems, a new era of intelligent and autonomous sensing applications emerges. The applications of AI-based optical sensors span across various industries, including biomedical and healthcare, environmental monitoring, manufacturing, and security. In the field of healthcare, these sensors contribute to medical diagnostics, disease and surgical monitoring, drug discovery, and personalized healthcare [10,11]. They enable non-invasive measurements, real-time monitoring of vital signs, and precise detection of biomarkers,

leading to improved patient care and early disease detection. In this research, we will explore AI-based optical sensors in healthcare applications, and more particularly, to improve AI solutions for disease detection.

### 1.1 Motivation

The coronavirus disease 2019 (COVID-19) pandemic's health support has greatly benefited from recent advancements in a number of fields, including AI and the health-related Internet of Things [12]. Travel restrictions have left people stranded, and a huge number of critically ill individuals have overloaded healthcare services. The epidemic is particularly dangerous to the elderly. As a result, both regular people and healthcare professionals are accustomed to in-home healthcare monitoring. Recent Internet of Nano Things (IoNT) devices use wearable and non-invasive off-the-shelf electronics to monitor physiological, emotional, activity-related, and vital states [13]. Additionally, it has been amazing to see how accurately AI systems have been able to read IoNT data [14]. DL algorithms, in particular, have developed as new types of AI algorithms that have demonstrated incredible accuracy in analyzing health-related data [15]. Modern DL algorithms can even instantly identify occurrences from Internet of medical things sensory data or live video feeds. A new generation of DL applications enabled by IoNT has been introduced as a result. One development in IoNT hardware, known as edge IoNT nodes, has made strides in the healthcare sector. Wherever it is necessary to monitor health data, such as at a hospital or at home, the current generation of IoNT nodes can be independently deployed. These edge health nodes now include a complete operating system with support for edge central processing units (CPUs) and graphics processing units (GPUs), enabling the node to carry out difficult DL computations at the edge. The edge learning and inferencing capabilities of DL applications have also been enhanced in order to take advantage of the development of advanced edge IoNT nodes. It is not necessary for data coming from a subject or hospital to leave the owner's area or edge; rather, DL and event monitoring can happen there. With the help of DL and the IoNT, this enables data privacy, security, and low-latency health apps to function on user premises. As a result, the edge IoNT has brought in new DL paradigms like federated learning, where learning occurs at the edge in a distributed manner while only the model is disseminated [16–18]. IoNT nodes that function as federated learning nodes can be supported by inexpensive GPU hardware.

Physical therapy [19], mobile-edge computing [20], and pandemic management [21], to name a few, are only a few of the health-related applications where IoNT has been deployed. However, DL has been widely used to combat COVID-19 in a variety of situations, including diagnosing COVID-19 from X-rays [22], computerized tomography (CT) scans [23], and diagnosing diabetic retinopathy [24]. Edge inferencing has been proposed to secure the privacy and security of IoNT data and to decrease the latency of IoNT inferencing. Another advancement is the proposal to facilitate edge learning with federated learning. Finally, IoNT and DL have been used to infer user emotional states and feelings. For instance, the IoNT was used to collect user sentiments. A DL sentiment analysis system that could comprehend a patient's emotional condition was created. Although the IoNT and DL have made significant strides, few have been applied in a context that supports various in-home quality-of-life monitoring situations within a single framework.

### 1.2 Contributions

To address the limitations of IoNT exploration in healthcare, we present the following contributions for our study:

1) We conducted research, implemented, and proposed several edge learning IoNT tools that can be employed to develop DL edge solutions.
2) We developed edge DL models for various IoNT devices, enabling the creation of health applications locally, including at home. Leveraging edge computing, our IoNT nodes can accommodate multiple DL-based models.
3) eXplainable artificial intelligence (XAI) is used to offer transparency and interpretability, enabling healthcare professionals to comprehend the reasoning behind the diagnostic decisions made by the designed model. This enhances trust in the automated diagnostic process.
4) Using IoNT edge learning, we developed various applications for measuring quality of life. They can track different phenomena and generate real-time notifications as well.

The rest of this article is divided into the following sections. We present a few closely comparable works in Section 2. We display the system's architecture and modeling in Section 3. The implementation details and the test results are presented and discussed in Section 4. Future directions are drawn in Section 5, and Section 6 concludes this article.

## 2 Related work

This section reviews the state-of-the-art solutions that are divided into two areas: IoNT and DL for disease detection.

## 2.1 IoNT

In order to increase the lifespan of wireless sensors networks in IoNT applications, a brand-new energy-efficient distributed routing technique has been developed [25]. All types of IoNT applications at the nanoscale can use the communication backbone of wireless sensor network built by choosing cluster head nodes in order to offer continuous data flow in crucial domains like healthcare operating *in vivo*. Chen *et al.* [26] pioneered the use of a novel feature to transmit the direction information in which molecules release themselves in IoNT environment. The performance of molecular communication systems is improved by releasing molecules in specific directions due to the reduction of multiuser interference. As a result, nearby transmitters can transmit data concurrently in several directions. For sensitive IoNT applications, such as those pertaining to healthcare, it then suggested the binary direction shift keying modulation system, in which the transmitter pumps molecules in two separate directions. Mangalwedhekar *et al.* [27] suggested a pulse position modulation-based energy-neutral event recognition framework, in which the event information is communicated by the sensors using the energy captured from the event. To identify transmitting nodes corresponding with a single receiver, it exploited pulse position. However, when a single node communicates with several receivers in IoNT networks without using an addressing scheme, it is also possible to do so using this strategy. In both situations, determining the event type is aided by the energy observation of the received pulse. Kim *et al.* [28] developed a computational formula and a probabilistic particle-based simulator to mimic chemical interaction with remarkable dynamical accuracy among dynamic nanorobots in the blood capillary and the neighboring cells. The transmitting bio-nanomachines produce data and are modeled as a rotating sphere with a continuous environmental pattern for a predetermined period of time. Blood flow characteristics are modeled, and their impact on the molecular received signal is investigated. An application of biomedical IoNT is also shown. Yadav *et al.* [29] displayed the designing of a protective circuit for electrocardiogram and electroencephalogram biomedical signals in the nano IoT. Any biomedical device must have a protection circuit, which is created using the Cadence Virtuoso environment in power supply. Defibrillator or electrostatic discharge-related events, such as voltage spikes and current spikes, are also analyzed. Owida *et al.* [30] evaluated the most recent research on the creation of carbon-based nanomaterials for biosensing, drug delivery, and cancer therapy. They also stressed the widely studied fundamental characteristics of carbon-based nanoparticles that are used to gather data on platforms for the IoNT. They noted that more thorough research is necessary to evaluate the toxicity and bioavailability of carbon-based nanomaterials because they still have some toxicity.

## 2.2 DL for disease detection

Bianco *et al.* [31] went through computer-aided diagnosis of hepatic lesions in light of localized and diffuse liver diseases. Ultrasonography, CT, and magnetic resonance imaging are the three main image capture modalities covered by the authors. Bianco *et al.* also gave the thoughtful analysis with benefits and drawbacks for each preliminarily phase, especially preprocessing, attribute analysis, and classification methods to carry out clinical diagnostic tasks. Their results revealed that convolutional neural networks based on DL deliver the best results. In order to provide a practical solution to this problem, Liu *et al.* [32] developed the ground-breaking area DL model. They started using shaped system with two paths while behind the final layer, which provides the required signed distance map, while another produces the target probability map. They then concentrated on the border of the target lesions or organs to be segmented with the aid of the signed distance map and acquired multi-scale features. They finally combined the region and boundary features in order to obtain the global results. A DL model for multi-classification study on infectious diseases is built based on actual hospital medical records of infectious disorders [33]. More than 20,000 cases of seven different infectious disease categories, including both inpatients and outpatients, are included in the data. Data normalization and sparse data processing are done through the auto-encoder to enhance the model training effect. For enhancing the learning process, a residual network and an attention mechanism are added. Lan [34] suggested performer, a cutting-edge transformer-based architecture that integrated the reconstructed ECG as various modalities for disease detection. They developed shifted patch-based attention (SPA), a powerful technique for encoding and decoding biological waveforms. The signal processing for both local features and global contextual representations is maximized by SPA through the retrieval of different sequence lengths and the capture of cross-patch linkages. In order to determine the statistical significance of K-fold cross-validation using statistical power and Type-I error rates, Jimenez-Mesa *et al.* [35] created a random-effects inference based on a label permutation test. The resulting framework made it possible to examine the generalizability of feature extraction techniques used in DL models. In a case–control study of Alzheimer's disease with proven results, a

hybrid feature extraction and classification model using support vector machines and autoencoders is assessed.

### 2.3 Discussion

This brief review of the literature highlights several limitations in current developments within IoNT for medical disease detection. One notable challenge is the critical issue of learning time computing, particularly in biomedical applications where nano hardware struggles to efficiently train developed models. Furthermore, there is a notable absence of an end-to-end framework for disease detection using nanorobots. To address these gaps, this study delves into the integration of nanorobots, DL, and edge computing within a unified embedded IoNT protocol. The aim is to tackle the challenges encountered in existing IoNT solutions. An application of this newly designed protocol on biomedical disease detection is also explored. The following section provides a comprehensive exploration of the proposed framework, detailing its components and functionality in depth.

## 3 Method design

### 3.1 Problem formulation

Let $X = \{x_1, x_2, \ldots, x_n\}$ denote a set of medical images, where $x_i$ represents an individual image. The goal is to develop a mathematical DL model that accurately detects the presence of diseases or abnormalities in these images. Let $Y = \{y_1, y_2, \ldots, y_n\}$ represent the set of the corresponding disease labels, where $y_i \in \{0, 1\}$ indicates the absence (0) or presence (1) of a disease for image $x_i$. The objective is to learn a DL model that maps each image $x_i$ to its corresponding disease label $y_i$. This model should generalize well to unseen images and accurately classify diseases based on the visual patterns present in the images. Given a training dataset $(X_{\text{train}}, Y_{\text{train}})$, the problem can be formulated as follows:

$$\min_{\theta} \mathcal{L}(\theta, X_{\text{train}}, Y_{\text{train}}),$$

where $\theta$ represents the model parameters, and $\mathcal{L}$ denotes the loss function. The training objective is to minimize the loss function $\mathcal{L}$, which measures the discrepancy between the predicted disease labels $\hat{y}$ and the ground truth labels $y$. The loss function can be defined as

$$\mathcal{L}(\theta, X_{\text{train}}, Y_{\text{train}}) = -\frac{1}{N_{\text{train}}} \sum_{i=1}^{N_{\text{train}}} (y_i \log(\hat{y}_i) + (1 - y_i) \log(1 - \hat{y}_i)),$$

where $N_{\text{train}}$ represents the number of samples in the training dataset. The model parameters $\theta$ are learned through an optimization algorithm, such as stochastic gradient descent, which updates the parameters based on the gradients of the loss function with respect to the parameters.

### 3.2 Principle

This section demonstrates the disease detection management system's intricate architecture. We exhibit the design along the following three dimensions to demonstrate the modular approach to the design (see Figure 1 for more details). We begin by demonstrating high-level applications that can be created using edge learning and the IoNT. The IoNT edge hardware that will enable us to support the applications is then determined. We then display the entire end-to-end stack, followed by our developed model that depicts the system's flow.

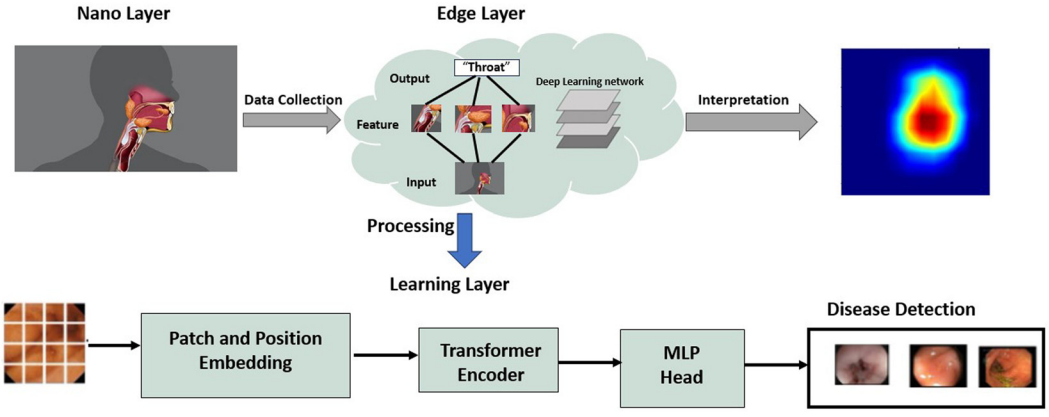


**Figure 1:** IoNT framework.

## 3.3 Nanorobot layer

Micro- and nanorobots may move individually or collectively. The driving mode has an effect on the movement speed, stability, and biocompatibility of micro/nanorobots, which has an effect on their employment in biological organisms. In order to overcome the challenges of low Reynolds fluid, the active motion of micro/nanorobots primarily relies on the conversion of a local chemical or muscular endurance.

1) Chemical propulsion: Adenosine triphosphate (ATP) is catalytically broken down in nature to provide intracellular propulsion by protein biomotors like myosin. In the past 10 years, a variety of micro/nanorobots that obtained the highest propulsion with chemical processes were inspired by them. The inert material is used to create the asymmetrical structure, and the catalyst's role is to interact with fuel on the robot's surface. $H_2O_2$ is the initial and most thoroughly studied fuel. In order to move, micro/nanorobots can generate their unique self-electrophoresis mechanisms and use materials like their own platinum (Pt) to catalyze the oxidation of $H_2O_2$ to make bubbles. High concentrations of $H_2O_2$ are hazardous to living beings. It is essential to create new *in situ* fuels besides $H_2O_2$ in order to accomplish practical applications, especially when chemical drive is employed to drive micro/nanorobots in living organisms. Organic elements that can be discovered in biological fluids should serve as the source ingredients. For instance, using biodegradable Zn or Mg, hydrogen can be produced by interacting with the acidic environment of the stomach to create self-propulsion and leaving left the same non-toxic result. Pt can also be substituted for an enzyme to form a catalytic process.
2) Physical propulsion: The majority of exterior field-driven micro- and nanorobots do not require fuel since these fields – light, ultrasonic, or magnetic – serve as their primary sources of propulsion. This offers them greater control over their movement and renders them biocompatible and sustainable. It is not too difficult to create stable conditions. Sonic waves can travel across solid, liquid, and air media to deeply penetrate biological tissue without endangering living things. They can use this to turn on micro- or nanorobots from outside. The light-driven micro/nanorobot is constructed mostly from photocatalytic, photorated, and photothermal materials. When exposed to light, these photoactive materials have the ability to absorb light energy and initiate photocatalytic, photopolymerization, and photothermal conversion processes. The magnetic field, along with other physical fields, can control the motion of micro- and nanorobots. We develop a reliable propulsion method that involves applying ultrasonic waves to the ground to reduce excess lateral drift during the entire motion so far as an electromagnetic field system is constructed to drive the spiral robot. This is a fresh and effective method for enhancing motion control.

## 3.4 Edge layer

We will create a collaborative training system with resource-constrained network edge to optimize the training acceleration offered by the dynamic task assignment. It focuses on delivering the training with the least amount of effort using only already-existing edge resources, whereas federated learning training is typically implemented using the cloud or a relatively centralized master node, which may result in additional hardware costs or communication overhead. In a cluster, the trade-off between compute power and communication capacity is carefully thought out and balanced. Each cluster is in charge of independently managing one DL task made up of many edge devices. Depending on the practical situation, they may be the same or different. A highly concentrated master node or the cloud's decentralized–centralized architecture may result in higher hardware costs or communication costs. In a cluster, there is careful consideration and a good balance between the processing resources and the communication constraints. The system elements in each cluster are described in the following manner:

1) Service parameters: Executors with a high communication requirement. They are in charge of maintaining new model parameters, receiving local gradients from worker, and storing model data. In order to engage, each service parameter links to every worker; however, there is no requirement for communication between service parameters. The service parameters used in this article differ from the standard service parameter notion in that it can be any device, including those with limited resources, as long as it can meet the needs for model update.
2) Workers: They get the most recent model from service parameters, train replicas of the model in parallel on local data (either distributed from associated service parameters or acquired locally), and submit intermediate results to service parameters. Each worker establishes a connection with every service parameter to upload gradients and download the most recent task. In asynchronous mode, the training model processed by each worker may differ slightly.

Because of the frequent exchanges between service parameters and workers, both parties need a lot of bandwidth.

The communication congestion caused by the weak node could prevent iteration update. In collaborative systems, resource management is a constant issue that is hardly ever addressed during edge-based training. The severe constraint in real-world applications is the weak network's resource-constrained edge devices' low computing, communication, and reliability capacities. It has motivated us to continue to demonstrate an effective solution to speed up collaborative training that can best balance the capabilities of different edge devices.

## 3.5 Learning layer

The field of medical image processing, as well as all other areas of information technology, saw a significant revolution thanks to AI. Objects in medical images were analyzed and identified using machine learning techniques. To recognize and analyze the items in medical images, a variety of DL approaches have become increasingly popular in recent years. Using DL techniques, disease detection can be identified in its early stages, assisting doctors in determining the best course of therapy. Although there is no cure for the illness, early discovery might slow its fast development. For early diagnosis, a variety of AI algorithms have been employed. DL techniques are a useful tool for assisting medical consultants in early disease detection. Based on DL techniques, the proposed learning system model accepts images retrieved from nanorobots that aid in the early detection and classification of diseases that may be in different stages. The training data, which comprised the data that were in raw form, were obtained from the nanorobot layer. The trained model is maintained in the edge-environment unless the learning requirements are satisfied, in which case the model should be retrained. The images that aid in the early diagnosis and classification of diseases that may be in their early stages are accepted by the proposed system model. Images gathered from sources are sent to the pre-processing worker during the validation phase. The images' dimensions are altered by the pre-processing worker. The suggested system model imports data from the edge for the intelligent classification after preprocessing is complete. If a patient exhibits symptoms of the condition, this intelligent system model detects and categorizes disease detection into four classes; otherwise, there is no need to see a doctor for disease detection treatment. In this research work, we will propose a new visual transformer for disease detection. Visual transformers have emerged as powerful models for disease detection tasks, leveraging their ability to capture long-range dependencies and contextual information in medical images. Here, we provide a detailed description of visual transformers for disease detection, including the model design and complexity analysis. Our visual transformer for disease detection consists of an encoder and a decoder. The encoder processes the input medical images to extract informative representations, while the decoder generates disease predictions based on these representations.

1. **Encoder** The encoder is composed of a stack of transformer encoder layers. Each encoder layer consists of multiple self-attention heads and feed-forward neural networks. The self-attention mechanism allows capturing relationships between different regions within the image. The encoder processes the input image $x$ and produces encoded image representations.

$$\text{Encoder}(x) = \text{TransformerEncoderLayer}(\text{LayerNorm}(x)),$$

where LayerNorm represents the layer normalization, and TransformerEncoderLayer applies self-attention and feed-forward networks. The self-attention mechanism involves calculating attention weights between different positions within the encoded image representations. Given an input representation $x_i$, the self-attention mechanism computes attention weights by attending to all other positions in the encoded image representation. The attention weights are then used to compute a weighted sum, representing the attended representation of $x_i$. The formulas for self-attention can be described as follows:

$$\text{Attention}(Q, K, V) = \text{softmax}\left(\frac{QK^T}{\sqrt{d_k}}\right)V,$$

where $Q$, $K$, and $V$ denote the queries, keys, and values, respectively. $d_k$ represents the dimensionality of the keys. The self-attention mechanism involves three linear transformations to obtain the query $Q$, key $K$, and value $V$ matrices:

$$Q = xW_Q, \quad K = xW_K, \quad V = xW_V,$$

where $W_Q$, $W_K$, and $W_V$ denote the learnable weight matrices.

2. **Decoder** The decoder takes the encoded image representations and generates disease predictions. It typically consists of fully connected layers followed by a softmax activation function. The decoder maps the encoded representations to the disease label space.

$$\text{Decoder}(x) = \text{Softmax}(\text{FC}(\text{Encoder}(x))),$$

where FC denotes the fully connected layers.

3. **Multi-scale attention mechanism** In our novel visual transformer, we introduce a multi-scale attention mechanism that enables the model to attend to different levels of detail in the medical images. This mechanism incorporates multiple self-attention layers, each focusing on a

specific scale of features. By attending to both local and global information, our model can effectively capture disease-related patterns at various scales. The multi-scale attention mechanism can be formulated as follows:

$$\text{Attention}^{(l)}(Q^{(l)}, K^{(l)}, V^{(l)}) = \text{softmax}\left(\frac{Q^{(l)}(K^{(l)})^T}{\sqrt{d_k}}\right)V^{(l)},$$

where $l$ denotes the layer index; $Q^{(l)}$, $K^{(l)}$, and $V^{(l)}$ represent the queries, keys, and values at layer $l$, respectively; and $d_k$ represents the dimensionality of the keys.

4. **Progressive refinement**: To improve the model's discriminative ability, we introduce a progressive refinement mechanism that iteratively refines the disease predictions. At each refinement step, the model leverages the information from both the original image and the refined predictions from the previous step. This progressive refinement allows the model to iteratively focus on disease-specific features and enhance the final disease detection performance.

The progressive refinement mechanism can be defined as:

$$\text{Refined\_Prediction}^{(t)} = \text{Decoder}(\text{Encoder}(x), \text{Refined\_Prediction}^{(t-1)}),$$

where $t$ represents the refinement step, Encoder and Decoder refer to the encoder and decoder modules, respectively, and $\text{Refined\_Prediction}^{(t-1)}$ denotes the refined predictions.

5. **Loss function**: To train our novel visual transformer, we employ a suitable loss function that encourages accurate disease classification. In addition to the conventional cross-entropy loss, we propose incorporating an auxiliary loss that promotes attention stability and encourages the model to focus on disease-specific regions. This auxiliary loss can be defined based on attention stability measures, such as the variance or entropy of the attention weights.

The overall loss function can be written as:

$$\mathcal{L} = \mathcal{L}_{\text{main}} + \lambda \cdot \mathcal{L}_{\text{aux}},$$

where $\mathcal{L}_{\text{main}}$ represents the main cross-entropy loss, $\mathcal{L}_{\text{aux}}$ denotes the auxiliary loss based on attention stability, and $\lambda$ is a weighting factor.

6. **Complexity analysis**. The complexity of visual transformers for disease detection depends on the number of layers, the size of each layer, and the number of self-attention heads. Let $L$ represent the number of transformer encoder layers, $H \times W$ denote the image size, and $D$ represent the dimensionality of the hidden representations.

a) **Encoding complexity:** The encoding step has a complexity of $O(L \cdot D^2 \cdot HW)$, as it involves self-attention and feed-forward neural networks.
b) **Decoding complexity:** The decoding step has a complexity of $O(D^2)$, as it consists of fully connected layers.
c) **Training complexity:** The training complexity depends on the number of parameters, which is influenced by the model size and architecture.
d) **Inference complexity:** The inference complexity depends on the number of layers, image size, and hidden representation dimensionality.

## 3.6 Hyper-parameter selection

The network can be prepared for training using a variety of elements, or other training options can be offered. Since they are not required for transfer learning, the final two layers of our visual transformer layers, SoftMax layers, and output classification layers, are not extracted. The learning rate, number of iterations, frequency of validation, and number of epochs can all be used as training choices. The network is trained with 39 iterations per epoch at a $1 \times 10^{-4}$ learning rate. Several epochs, including 100, 200, 300, and 400, were used for training. The stochastic gradient descent with momentum (SGDM) optimization technique is used for training. These training settings enable newly updated layers to incorporate the disease detection dataset's features. Different epochs, including 100, 200, 300, and 400, were evaluated for the training of the transfer learning algorithm, and it was found that epoch 400 was the best. The best learning rate was found to be $1 \times 10^{-4}$ after varying the learning rate between $1 \times 10^{-1}$ and $1 \times 10^{-5}$. To reach the required level of precision, the algorithm was repeatedly retrained to achieve maximum accuracy.

## 3.7 Interpretation

We utilized the XAI technique known as gradient-weighted class activation mapping (Grad-CAM) to provide insights into our DL model's for disease detection. Grad-CAM helps us understand which regions of the input image contribute the most to the model's prediction. To gain a better understanding of how our model is making predictions, we generated activation maps using Grad-CAM. These maps highlight the regions of the input image that the model found most important in making its diagnosis. The Grad-CAM score $S_c$ for a particular class $c$ at a given spatial location can be calculated as follows:

$$S_c(x, y) = \sum_k \alpha_{c,k} A_k(x, y), \quad (1)$$

where $S_c(x, y)$ represents the Grad-CAM score at position $(x, y)$, $\alpha_{c,k}$ is the weight of the last convolutional layer's

feature map $k$ for class $c$. $A_k(x, y)$ is the activation of feature map $k$ at position $(x, y)$. The interpretation of these Grad-CAM activation maps is invaluable for clinical practitioners. It allows them to not only trust the model's predictions but also understand the basis for those predictions. For example, in the case of lung disease detection, the activation maps may reveal that the model is primarily looking at specific lung nodules or abnormalities, which can aid radiologists in confirming the diagnosis. Additionally, Grad-CAM can help assess the model's confidence and uncertainty. If the activation maps indicate that the model is focused on the relevant disease markers, it can increase confidence in the diagnosis. Conversely, if the model's attention is scattered or focused on irrelevant areas, this information can be used to assess the uncertainty associated with the prediction. We can express the model's uncertainty $U$ as a function of the Grad-CAM scores:

$$U(x, y) = 1 - \frac{S_c(x, y)}{\sum_{c'} S_{c'}(x, y)}, \tag{2}$$

where $U(x, y)$ represents the uncertainty at position $(x, y)$, and $S_c(x, y)$ is the Grad-CAM score for class $c$ at that position. Incorporating XAI techniques like Grad-CAM into disease detection models not only enhances transparency but also aids in clinical interpretation. It provides valuable insights into the model's decision-making process, highlighting the regions of interest in medical images, and allows for the quantification of uncertainty, ultimately improving trust and utility in AI-assisted medical diagnostics.

# 4 Performance evaluation

## 4.1 Implementation details

NVIDIA (NVIDIA Corporation, USA) introduced the Jetson Nano, a compact, potent computer for embedded AI applications including edge computing and robotics, in March 2019. With a Qued-core ARM Cortex-A57 CPU and a 128-core GPU built on the MAXwell architecture, it can provide enough processing power for AI applications like biomedical applications. Additionally, thanks to NVIDIA's generous provision of DL interfaces, the Jetson Nano has evolved into the perfect embedded platform for edge computing. It supports several well-known AI frameworks and algorithms, including PyTorch, Caffe, MXNet, and NVIDIA's CUDA, cuDNN, and TensorRT software libraries. The standard power supply that NVIDIA controls is 4A@5V, which satisfies the trained model's power supply needs. On the Jetson Nano, computer vision tasks can be supported by both CSI and USB cameras. Jetson Nano, however, is a superb embedded developer kit that satisfies the hardware requirements for model deployment. We used Jetson Nano in our implementation for the developed system. To verify the applicability of IoNR-DD in disease detection, we used the Kvasir medical database [36]. The goal is to automatically detect endoscopic findings in the rectum, esophagus, stomach, and intestines. There are two versions of it. Kvasir (v1), the original edition, has 4,000 available data divided into eight classifications that represent anatomical landmarks, diseased abnormalities, or endoscopic procedures. The second called Kvasir (v2) builds upon the first and has 8,000 available data and the same amount of classes. This dataset is used to evaluate the edge layer and the learning layer for the IoNR-DD framework. In order to evaluate the nano robotics layer, we used practical health readings obtained from the online MIMIC benchmark.[1]

The accuracy and $F1$ formulas are used to determine the IoNR performance. They are described in the following:

$$F1 = \frac{2 \times \text{Precision} \times \text{Recall}}{\text{Precision} + \text{Recall}}, \tag{3}$$

$$\text{Accuracy} = \frac{\text{TP} + \text{TN}}{\text{TP} + \text{TN} + \text{FN} + \text{FP}}, \tag{4}$$

$$\text{Precision} = \frac{\text{TP}}{\text{TP} + \text{FP}}, \tag{5}$$

$$\text{Recall} = \frac{\text{TP}}{\text{TP} + \text{FN}}. \tag{6}$$

The following are definitions of the notations used in the aforementioned equations:

1) True positive (TP): The number of observations with corrected positive results is counted to determine it. If and only if an observation is an endoscopic discovery that the running model also recognizes, it is referred to as a correct positive.
2) True negative (TN): The number of rectified negative observations is counted to determine it. If and only if an observation is not an endoscopic discovery and is regarded as such by the running model, it is said to be correct negative.
3) False positive (FP): By counting the instances of falsely positive observations, it is calculated. If and only if an observation is an endoscopic discovery and the running model classifies it as a non-endoscopic finding, it is referred to as a false positive.

1 https://github.com/YerevaNN/mimic3-benchmarks

4) False negative (FN): By counting the amount of false negative observations, it can be calculated. If and only if an observation does not match the running model's definition of an endoscopic discovery, it is referred to as a false negative.

## 4.2 Nanorobot-layer performance

To evaluate the nanorobots layer, an intensive simulation on MIMIC has been carried out. Figure 2 demonstrates the energy consumption of nodes responsible for collecting medical data, specifically focusing on the respiration rate within the MIMIC dataset. It is assumed that each node operates within an energy range set between 650 and 750 units. Each measurement that is sent or collected uses 0.3 and 1 units, respectively. Over 24 periods, the values correspond to a typical patient (40 min). We compared IoNR-DD with nanorobot layer with local emergency detection (LED) [37] and modified LED [38]. With *alpha* = 0.05, we allow all three algorithms to adjust the node's sampling rate to the dynamic evolution of the respiration rate. Since the transmission is optimized, the proposed solution consumes less energy compared to both enhanced LED and LED technologies. Our algorithm demonstrates energy savings of up to twice as much when compared to LED and enhanced LED methods. These results are attributed to the efficient nanorobot developed in this research, using both chemical and physical propulsion techniques.

## 4.3 Edge-layer performance

To evaluate the edge layer, the training runtime is determined using Kvasir data. Figure 3 presents the training time for both Kvasir (V1) and Kvasir (V2) where duplicating the size to 1 time, 10 times, 100 times, and 1,000 times. We train the DL model proposed in IoNR-DD in a single computer and also in edge computing hardware. The results reveal the clear superiority of the edge-based solution compared to the single computer-based configuration. Indeed, using edge-based solution, 20 h is needed to train the eight million images of 1,000 times of Kvasir dataset, where the single computer needs more than 10 days to train the same amount of data. This result clearly demonstrates the necessity of using edge layer in IoNR-DD.

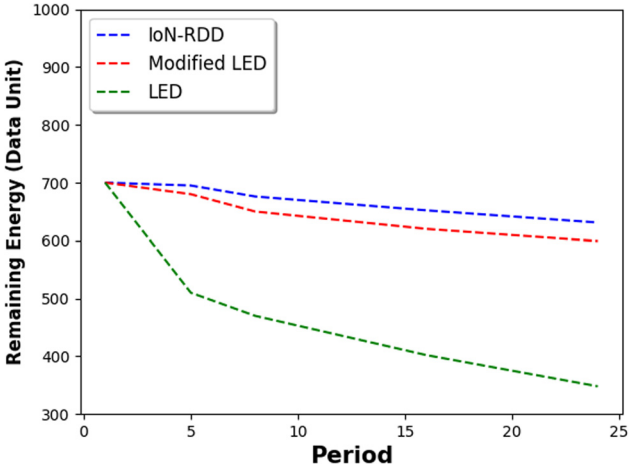


**Figure 2:** Runtime of data collection of IoNR-DD *versus* advanced medical data collection-based solutions.

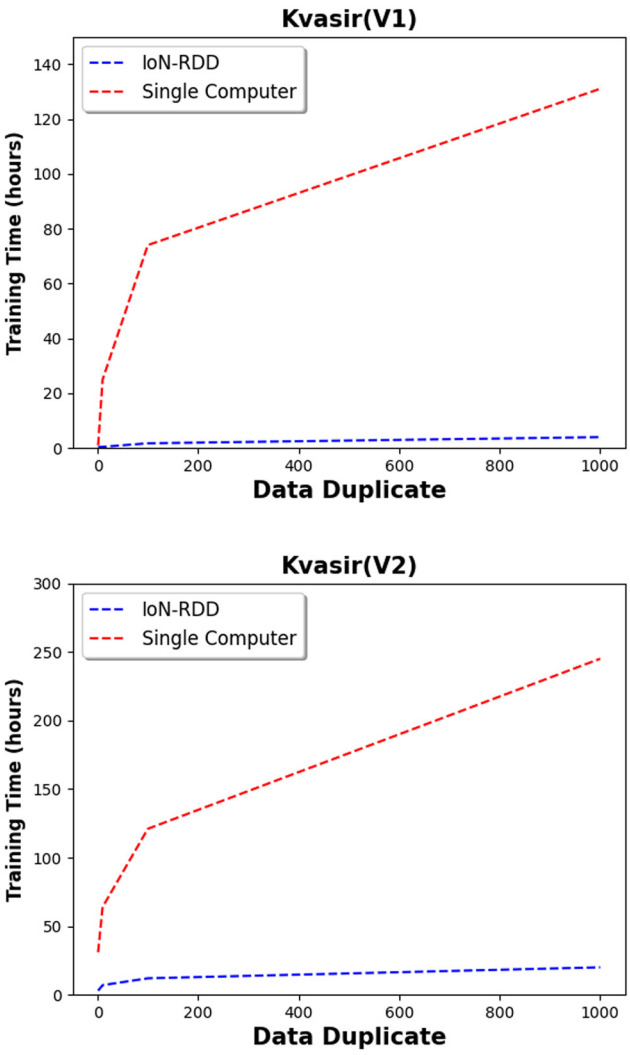


**Figure 3:** Runtime of training of IoNR-DD *versus* advanced edge-based solutions.

## 4.4 Learning-layer performance

Table 1 depicts the IoNR-DD results' quality along with the standard solutions including ALMOST [10], InceptionResNet

**Table 1:** IoNR-DD *vs* disease detection baseline strategies

| Data.\|Images\| | IoNR-DD | | ALMOST | | InceptionResNet | | DenseNet | |
|---|---|---|---|---|---|---|---|---|
| | *F*1 | Accuracy | *F*1 | Accuracy | *F*1 | Accuracy | *F*1 | Accuracy |
| Kvasir(V1).1000 | 0.55 | 0.58 | 0.53 | 0.57 | 0.48 | 0.51 | 0.47 | 0.49 |
| Kvasir(V1).2000 | 0.56 | 0.60 | 0.56 | 0.59 | 0.50 | 0.53 | 0.50 | 0.51 |
| Kvasir(V1).3000 | 0.59 | 0.64 | 0.58 | 0.63 | 0.52 | 0.55 | 0.52 | 0.53 |
| Kvasir(V1).4000 | 0.64 | 0.66 | 0.63 | 0.66 | 0.55 | 0.58 | 0.54 | 0.54 |
| Kvasir(V2).1000 | 0.56 | 0.63 | 0.57 | 0.62 | 0.56 | 0.56 | 0.53 | 0.54 |
| Kvasir(V2).2000 | 0.66 | 0.69 | 0.64 | 0.66 | 0.59 | 0.60 | 0.54 | 0.57 |
| Kvasir(V2).3000 | 0.71 | 0.75 | 0.69 | 0.73 | 0.60 | 0.60 | 0.58 | 0.61 |
| Kvasir(V2).4000 | 0.76 | 0.78 | 0.75 | 0.77 | 0.65 | 0.69 | 0.63 | 0.64 |
| Kvasir(V2).5000 | 0.81 | 0.88 | 0.80 | 0.84 | 0.68 | 0.72 | 0.65 | 0.67 |
| Kvasir(V2).6000 | 0.86 | 0.88 | 0.83 | 0.86 | 0.72 | 0.74 | 0.66 | 0.69 |
| Kvasir(V2).7000 | 0.85 | 0.92 | 0.87 | 0.91 | 0.75 | 0.77 | 0.71 | 0.72 |
| Kvasir(V2).8000 | 0.94 | 0.99 | 0.92 | 0.96 | 0.77 | 0.79 | 0.72 | 0.75 |

[39], and DenseNet [40] on Kvasir (V1) and Kvasir (V2). For Kvasir (V1) and Kvasir (V2), we changed the percentage of images used for training from 1,000 to 4,000 and from 1,000 to 8,000, respectively. The accuracy and quality of the outcomes as represented by the *F*1 formulas are then calculated. The outcomes demonstrate IoNR-DD's superiority to the baseline solutions in almost all cases. As a result, IoNR-DD's accuracy achieved 0.99 when all of the Kvasir (V2) data are processed. This could be achieved by the other solutions where the accuracy of the InceptionResNet, and DenseNet solutions is less than 0.80, and the accuracy of ALMOST is 0.96 for the same data used in the training. These outcomes are made possible by the efficient adaptation of the visual transformers with the novel attention mechanism employed in this research work, where the most relevant features of all image channels are used in the learning phase.

### 4.5 XAI performance

Figure 4 presents the GradCam [41,42] of IoNR-DD solution on Ksavir dataset. From this figure, we can conclude that using Grad-CAM for disease detection is an exciting and promising application of DL in the field of medical imaging and diagnostics. It allows us to visualize and understand which regions of an image are most influential in a neural network's decision-making process, making it valuable for interpreting and improving the transparency of DL models in medical contexts. It illustrates how the regions highlighted by Grad-CAM fit very well to the mask of the diseases in the images. In fact, it provides a level of interpretability and transparency in IoNR-DD that is crucial in medical applications. Doctors and healthcare professionals need to understand why IoNR-DD makes a certain prediction, and Grad-CAM helps by highlighting the regions in an image that contribute the most to the IoNR-DD model's decision. This can help build trust in the IoNR-DD model's predictions. It is often essential to pinpoint the exact location of a disease or anomaly within an image. Grad-CAM can be used to create heatmaps that highlight the areas where the model believes the disease is present. This assists radiologists and clinicians in focusing their attention on these regions for further analysis.

## 5 Potential research challenges

The majority of the biomedical-based applications we use in our daily lives, including body sensors, are incorporating IoNT. These gadgets are connected to the Internet and have digitalized control and monitoring processes, which presents various security and privacy concerns. A completely new level of security-related difficulties is brought by the incorporation of body area networks systems with body devices and nano machineries. The security of data transmitted over the internet is one of the most significant difficulties brought on by the expansion of the market for the IoNT. Additionally, a completely new level of security-related difficulties are brought about by the integration of body area networks systems with body devices and nano machineries. The security of data transmitted over the Internet is one of the most significant difficulties brought on by the expansion of the market for the IoNT. Personal health information can be stolen by a bio-cyber attack in the healthcare industry. This knowledge can be used to develop new virus kinds that can penetrate already-installed nanosensors in IoNT. In order to avoid these issues, communication networks in the

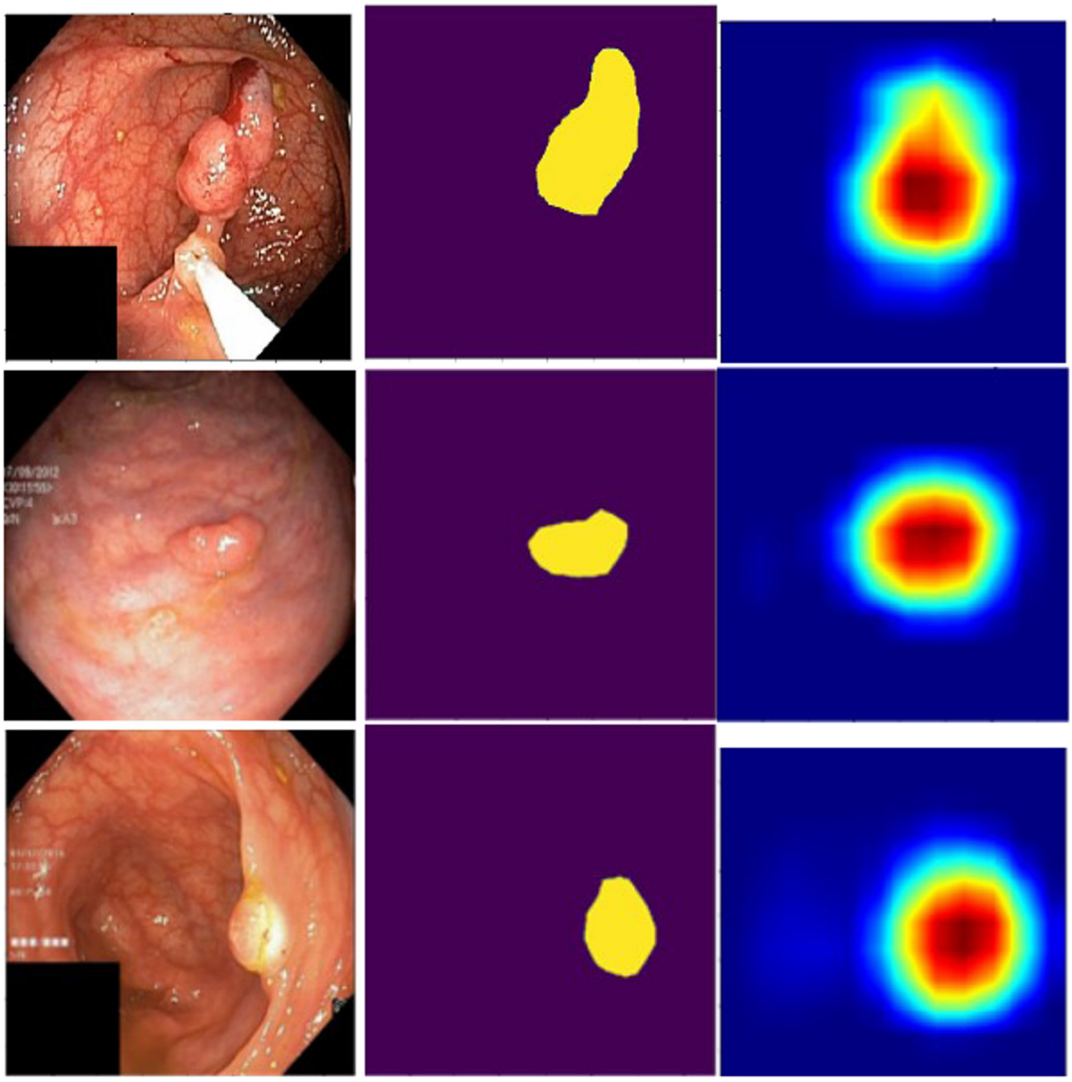

**Figure 4:** GradCam of IoNR-DD solution.

4G and 5G eras, particularly in IoNT, should employ security assurance approaches while carefully taking into account the nature of IoNT communications. Concerns about privacy and security must be addressed since nanodevices collect significant amounts of sensitive data. It is important for users of IoNT infrastructure to be aware of who will have access to their data and how it will be used. A secure site must be used to keep the obtained data, and cutting-edge cyber-security methods must be used. If left unattended, cybercriminals may gain unauthorized access to this private information. Users may be interested in finding out who might be held accountable for a cyber-security assault and what mitigating measures can be taken. Therefore, before IoNT devices are mass produced and used, these difficulties need to be taken into account by IoNT developers. A significant obstacle in the development of biomedical nanosensors is compatibility. The bodies of patients should not be adversely affected by these microsensors, and they must support continuous connectivity with wearable technology, according to developers. Designers and developers may need to look for and investigate a wide variety of materials that can be suitable with the human body for this purpose. However, locating such materials will necessitate considerable testing, which will add time and risk of error to the process. A high level of precision of the proposed system in this research work is achieved by the efficient fusion of intelligent technologies in the form of DL, edge computing, and nanorobots. However, inference runtime performance is still an issue for real-time disease detection. The creation of hybrid systems that combine advanced DL [43,44], decomposition [45], and optimization [46] to enhance the performance of the developed system in this research work could be a promising direction. Exploring efficient data

representation to efficiently learn from multi-modalities might also result in systems with high precision [47].

# 6 Conclusion

In this study, we show the fusion of DL and nanotechnology, which presents an exciting opportunity to revolutionize crucial aspects of nanoscience and technology. This partnership has the potential to catalyze significant breakthroughs in crafting innovative materials, devising cutting-edge devices, and developing transformative applications, unleashing unprecedented possibilities. In this sense, we developed a framework for intelligent computing leveraging the IoNT deployed in user-edge environments. Using edge nodes, we facilitated the collection and generation of alerts for various disease detection issues by deploying cutting-edge DL applications at the edge. This approach ensures user data privacy, security, and low latency through an edge-computing architecture. Additionally, XAI was employed to enhance trust by offering transparent insights into our model's decision-making process, empowering clinicians to comprehend and validate diagnostic outcomes effectively, thereby enhancing patient care. The provision of in-home healthcare and symptom management represents a crucial advancement in healthcare support, particularly amidst pandemics where access to specialist physicians is limited and travel restrictions are imposed, especially impacting the elderly population. The results on Kvasir dataset validated the applicability of the proposed solution compared to the state-of-the-art disease detection-based methods.

**Funding information:** The authors state no funding involved.

**Author contribution:** All authors have accepted responsibility for the entire content of this manuscript and approved its submission.

**Conflict of interest:** The authors state no conflict of interest.

**Data availability statement:** The datasets generated and/or analysed during the current study are available from the corresponding author on reasonable request.

# References

[1] Ruiz Euler HC, Boon MN, Wildeboer JT, van de Ven B, Chen T, Broersma H, et al. A deep-learning approach to realizing functionality in nanoelectronic devices. Nature Nanotechnol. 2020;15(12):992–8.

[2] Pimenov DY, Gupta MK, da Silva LR, Kiran M, Khanna N, Krolczyk GM. Application of measurement systems in tool condition monitoring of Milling: A review of measurement science approach. Measurement. 2022;199:111503.

[3] Selvarajan S, Manoharan H, Iwendi C, Al-Shehari T, Al-Razgan M, Alfakih T. SCBC: smart city monitoring with blockchain using Internet of things for and neuro fuzzy procedures. Math Biosci Eng. 2023;20(12):20828–51.

[4] Selvarajan S, Manoharan H, Shankar A. SL-RI: Integration of supervised learning in robots for industry 5.0 automated application monitoring. Measurement Sensors. 2024;31:100972.

[5] Zheng C, An Y, Wang Z, Qin X, Eynard B, Bricogne M, et al. Knowledge-based engineering approach for defining robotic manufacturing system architectures. Int J Production Res. 2023;61(5):1436–54.

[6] Sabato A, Dabetwar S, Kulkarni NN, Fortino G. Non-contact sensing techniques for AI-aided structural health monitoring: a systematic review. IEEE Sensors J. 2023;23:4672–84.

[7] Liu XF, Zhu HH, Wu B, Li J, Liu TX, Shi B. Artificial intelligence-based fiber optic sensing for soil moisture measurement with different cover conditions. Measurement. 2023;206:112312.

[8] Zou Y, Zhong M, Li S, Qing Z, Xing X, Gong G, et al. Flexible wearable strain sensors based on laser-induced graphene for monitoring human physiological signals. Polymers. 2023;15(17):3553.

[9] Zhang A, Zhang S. High stability fiber-optics sensors with an improved PGC demodulation algorithm. IEEE Sensors J. 2016;16(21):7681–4.

[10] Djenouri Y, Belhadi A, Yazidi A, Srivastava G, Chatterjee P, Lin JCW. An intelligent collaborative image-sensing system for disease detection. IEEE Sensors J. 2022;23:947–54.

[11] Lu S, Yang J, Yang B, Li X, Yin Z, Yin L, et al. Surgical instrument posture estimation and tracking based on LSTM. ICT Express. 2024.

[12] Zhao Z, Li X, Luan B, Jiang W, Gao W, Neelakandan S. Secure Internet of things (IoT) using a novel Brooks Iyengar quantum Byzantine agreement-centered blockchain networking (BIQBA-BCN) model in smart healthcare. Inform Sci. 2023;629:440–55.

[13] Ghildiyal Y, Singh R, Alkhayyat A, Gehlot A, Malik P, Sharma R, et al. An imperative role of 6G communication with perspective of industry 4.0: challenges and research directions. Sustain Energy Technol Assessments. 2023;56:103047.

[14] Alam MU, Rahmani R. FedSepsis: a federated multi-modal deep learning-based Internet of medical things application for early detection of sepsis from electronic health records using Raspberry Pi and Jetson Nano devices. Sensors. 2023;23(2):970.

[15] Ben Ameur H, Boubaker S, Ftiti Z, Louhichi W, Tissaoui K. Forecasting commodity prices: empirical evidence using deep learning tools. Ann Operat Res. 2023:1–19.

[16] Yang Q, Huang A, Fan L, Chan CS, Lim JH, Ng KW, et al. Federated learning with privacy-preserving and model IP-right-protection. Machine Intelligence Res. 2023;20(1):19–37.

[17] Farahani B, Monsefi AK. Smart and collaborative industrial IoT: A federated learning and data space approach. Digital Commun Netw. 2023;9(2):436–47.

[18] Chahoud M, Otoum S, Mourad A. On the feasibility of Federated Learning towards on-demand client deployment at the edge. Inform Process Manag. 2023;60(1):103150.

[19] Fulk G. Artificial intelligence and neurologic. J Neurol Phys Therapy. 2023;47(1):1–2.

[20] Li S, Li C, Huang Y, Jalaian BA, Hou YT, Lou W. Enhancing resilience in mobile edge computing under processing uncertainty. IEEE J Selected Areas Commun. 2023;41:659–74.
[21] Oktari RS, Latuamury B, Idroes R, Sofyan H, Munadi K. Knowledge management strategy for managing disaster and the COVID-19 pandemic in Indonesia: SWOT analysis based on the analytic network process. Int J Disaster Risk Reduction. 2023;85:103503.
[22] Ullah Z, Usman M, Gwak J. MTSS-AAE: multi-task semi-supervised adversarial autoencoding for COVID-19 detection based on chest X-ray images. Expert Syst Appl. 2023;216:119475.
[23] Hayat A, Baglat P, Mendonça F, Mostafa SS, Morgado-Dias F. Novel Comparative Study for the Detection of COVID-19 Using CT Scan and Chest X-ray Images. Int J Environ Res Public Health. 2023;20(2):1268.
[24] Bhattacharjee R, Mishra A, Mishra C, Bhawsinka Y. Chronic myeloid leukemia diagnosed from the course of diabetic retinopathy. Med J Armed Forces India. 2023.
[25] Gulec O, Sahin E. Red Deer algorithm based nano-sensor node clustering for IoNT. J Netw Comput Appl. 2023;213:103591.
[26] Chen X, Ji F, Wen M, Huang Y, Tang Y, Eckford AW. Low complexity first: duration-centric ISI Mitigation in molecular communication via diffusion. IEEE Commun Lett. 2022;26(11):2665–9.
[27] Mangalwedhekar R, Singh N, Thakur CS, Seelamantula CS, Jose M, Nair D. Achieving nanoscale precision using neuromorphic localization microscopy. Nature Nanotechnol. 2023;18:1–10.
[28] Kim SJ, Singh P, Jung SY. A machine learning-based concentration-encoded molecular communication system. Nano Commun Netw. 2023;35:100433.
[29] Yadav P, Bansod P, Mishra D, Jarwal R. Design of protection circuit for biomedical signals using 180 nm technology. In: Microelectronics, communication systems, machine learning and Internet of things. Singapore: Springer; 2023. p. 165–76.
[30] Owida HA, Turab NM, Al-Nabulsi J. Carbon nanomaterials advancements for biomedical applications. Bulletin Electr Eng Inform. 2023;12(2):891–901.
[31] Bianco A, Al-Azzawi ZA, Guadagno E, Osmanlliu E, Gravel J, Poenaru D. Use of machine learning in pediatric surgical clinical prediction tools: A systematic review. J Pediatric Surgery. 2023;58:908–16.
[32] Liu W, Liu X, Luo X, Wang M, Han G, Zhao X, et al. A pyramid input augmented multi-scale CNN for GGO detection in 3D lung CT images. Pattern Recognit. 2023;136:109261.
[33] Wang M, Wei Z, Jia M, Chen L, Ji H. Deep learning model for multi-classification of infectious diseases from unstructured electronic medical records. BMC Med Inform Decision Making. 2022;22(1):1–13.
[34] Lan E. Performer: a novel PPG-to-ECG reconstruction transformer for a digital biomarker of cardiovascular disease detection. In: Proceedings of the IEEE/CVF Winter Conference on Applications of Computer Vision; 2023. p. 1991–9.
[35] Jimenez-Mesa C, Ramirez J, Suckling J, Vöglein J, Levin J, Gorriz JM, et al. A non-parametric statistical inference framework for deep learning in current neuroimaging. Inform Fusion. 2023;91:598–611.
[36] Pogorelov K, Randel KR, Griwodz C, Eskeland SL, de Lange T, Johansen D, et al. Kvasir: A multi-class image dataset for computer aided gastrointestinal disease detection. In: Proceedings of the 8th ACM on Multimedia Systems Conference; 2017. p. 164–9.
[37] Elghers S, Makhoul A, Laiymani D. Local emergency detection approach for saving energy in wireless body sensor networks. In: 2014 IEEE 10th International Conference on Wireless and Mobile Computing, Networking and Communications (WiMob). IEEE; 2014. p. 585–91.
[38] Habib C, Makhoul A, Darazi R, Salim C. Self-adaptive data collection and fusion for health monitoring based on body sensor networks. IEEE Trans Industr Inform. 2016;12(6):2342–52.
[39] Wang Y, Jing C, Huang W, Jin S, Lv X. Adaptive spatiotemporal InceptionNet for traffic flow forecasting. IEEE Trans Intelligent Transport Syst. 2023;24:3882–907.
[40] Bui TH, Hoang VM, Pham MT. Automatic varied-length ECG classification using a lightweight DenseNet model. Biomed Signal Process Control. 2023;82:104529.
[41] Raghavan K. Attention guided grad-CAM: an improved explainable artificial intelligence model for infrared breast cancer detection. Multimedia Tools Appl. 2023:1–28.
[42] Viswan V, Shaffi N, Mahmud M, Subramanian K, Hajamohideen F. Explainable artificial intelligence in Alzheimer's disease classification: a systematic review. Cognitive Comput. 2024;16(1):1–44.
[43] Cong R, Sheng H, Yang D, Cui Z, Chen R. Exploiting spatial and angular correlations with deep efficient transformers for light field image super-resolution. IEEE Trans Multimedia. 2023.
[44] Lin Q, Xiongbo G, Zhang W, Cai L, Yang R, Chen H, et al. A novel approach of surface texture mapping for cone-beam computed tomography in image-guided surgical navigation. IEEE J Biomed Health Inform. 2023.
[45] Djenouri Y, Hatleskog J, Hjelmervik J, Bjorne E, Utstumo T, Mobarhan M. Deep learning based decomposition for visual navigation in industrial platforms. Appl Intell. 2022;52:1–17.
[46] Djenouri Y, Belhadi A, Srivastava G, Lin JCW. Hybrid graph convolution neural network and branch-and-bound optimization for traffic flow forecasting. Future Generation Comput Syst. 2023;139:100–8.
[47] Djenouri Y, Belhadi A, Lin JCW, Djenouri D, Cano A. A survey on urban traffic anomalies detection algorithms. IEEE Access. 2019;7:12192–205.